Cross-linking of Aqueous Base-Developable, Photosensitive Polynorbornene

Mehrsa Raeis-Zadeh,[1] Ed Elce,[2] Brian Knapp,[2] Paul A. Kohl[1]

[1]*School of Chemical and Biomolecular Engineering, Georgia Institute of Technology, Atlanta, Georgia*
[2]*Promerus LLC, Brecksville, Ohio*

Received 2 February 2010; accepted 21 August 2010
DOI 10.1002/app.33273
Published online 7 December 2010 in Wiley Online Library (wileyonlinelibrary.com).

ABSTRACT: The effect of epoxy-based cross-linking additives with different functionalities on the photolithographic properties, adhesion to substrates, and cross-link density of a tetramethyl ammonium hydroxide-developable polynorbornene-based dielectric was investigated. Three different multifunctional epoxy additives were investigated: difunctional, trifunctional, and tetrafunctional compounds. It was found that incorporation of a small quantity (1 wt % of solution) of an ultraviolet-absorbing tetrafunctional cross-linker, tetraphenylol ethane tetraglycidyl ether, activated the photo-catalyst and improved the sensitivity of a previously photosensitive polynorbornene-based formulation by a factor of 3.7. The impact of the epoxy cross-linkers on the physical and optical properties of the polymer formulations was evaluated. The contrast was improved from 7.37, for the control formulation, to 24.2. The polymer-to-substrate adhesion was also improved by addition of the tetrafunctional epoxy cross-linker, which facilitates the development of high-aspect-ratio structures. Hollow-core pillar structures in 40-μm-thick films with a depth-to-width aspect ratio of 13 : 1 were produced. The cross-link density was studied by using swelling measurements of cured films to evaluate the average molecular weight between cross-links. © 2010 Wiley Periodicals, Inc. J Appl Polym Sci 120: 1916–1925, 2011

Key words: epoxy resins; cross-link functionality; cross-link density; light absorptivity; photodefinition properties; high-aspect-ratio structures

INTRODUCTION

Polymer materials are widely used in microelectromechanical system (MEMS) and microelectronics packaging.[1–3] Numerous photosensitive and nonphotosensitive polymers have been developed for MEMS applications.[4–11] Epoxy-based polymers are of special interest because they can have excellent adhesion to substrates and modest cure temperatures.[1] Furthermore, several studies of photodefinable, high-aspect-ratio materials have recently been reported.[1,4,12-14] Among the most desirable attributes for photosensitive polymers is the ability to achieve high-aspect-ratio (depth-to-width) structures with excellent adhesion and high sensitivity. The acid catalyzed activation of epoxy groups is an efficient way to achieve cross-linking and enhance the polymer properties, especially adhesion.[4] For example, SU-8 (Micro-Chem Corp., MCC, Newton, MA), a negative-tone, solvent-developable epoxy-based formulation, first developed at IBM, has been used extensively for making high-aspect-ratio MEMS device structures and packaging components.[8,12,15–18] SU-8 shows high mechanical strength[19] and thermal stability and low susceptibility to swelling during developing because of its high cross-link density.[12,14] However, processing of SU-8 is a challenging task because it is sensitive to the processing conditions and variations.[5,20–26]

Previously, Rajarathinam et al.[1] have shown that an epoxy cross-linked polynorbornene (PNB) polymer formulation has straightforward processing parameters. High-contrast formulations (contrast = 12.2) were developed in aqueous-base. The contrast (γ) of the polymer was obtained by measuring film thickness after developing as a function of exposure dose.[1] The contrast was defined by eq. (1).[27]

$$\gamma = \frac{1}{log_{10}\frac{D_{100}}{D_0}} \qquad (1)$$

where D_{100} is the minimum exposure dose where none of the photodefined material is removed after exposure and developing, and D_0 is the maximum exposure dose where all of the polymer is soluble and removed during developing.

High-fidelity features with aspect ratios of 7 : 1, and vertical side-walls were fabricated in thick

Correspondence to: P. A. Kohl (paul.kohl@chbe.gatech.edu).

© 2010 Wiley Periodicals, Inc.

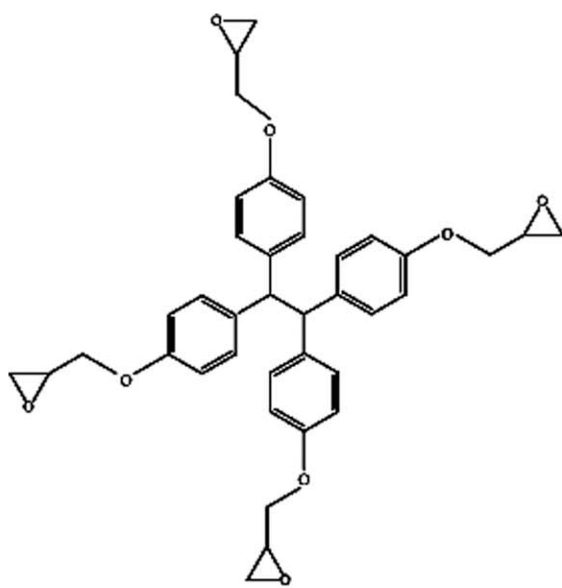

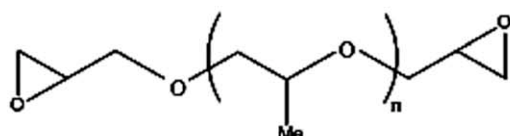

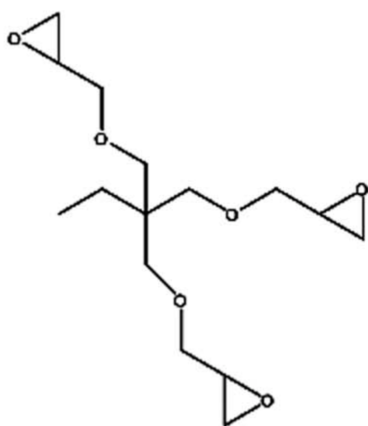

Figure 1 The chemical structure of (a) tetraphenylol ethane tetraglycidyl ether, I; (b) polypropylene glycol diglycidyl ether, II; and (c) trimethylolpropane triglycidyl ether, III.

films.[1] The PNB formulation with a high epoxy content showed comparable mechanical strength and residual stress to SU-8. The elastic modulus and hardness were reported as 2.9 and 0.18 GPa, respectively, for the fully cross-linked films.[1] The elastic modulus for SU-8 is 3.3 GPa.[1] The hardness (H) was defined as the applied load per unit area of indentation, as given by eq. (2).[28]

$$H = \frac{P_{\max}}{A(h_c)} \tag{2}$$

where $P_{\max}$ is the maximum load, and the projected contact area, $A(h_c)$, for an indenter with a tip imperfection was defined by eq. (3).

$$A(h_c) = 24.5h_c^2 + \sum_{i=0}^{7} a_i h_c^{1/2^i} \tag{3}$$

where h_c was estimated for a geometrical constant (ε) by using the Oliver and Pharr model, eq. (4).

$$h_c = h_{\max} - \varepsilon \frac{P_{\max}}{S} \tag{4}$$

In this work, the effect of different epoxy-based cross-linkers on the physical and photochemical properties of a PNB-based dielectric was investigated, in an effort to enhance the resolution, aspect ratio, adhesion, and photo-speed. The base polymer formulation (BF) used in this study was the same as that of Rajarathinam et al.,[1] and the results were compared with the results reported previously. The structures of the epoxy-based cross-linkers used in this study are shown in Figure 1 and will be identified as I, II, and III hereafter. The BF used in this study was prepared from a functionalized PNB polymer, as shown in Figure 2. Carboxylic acid groups on the polymer backbone provided cross-linking sites for the epoxy. The PNB polymer was mixed with different ratios of II and III to form a polymer formulation (BF), which replicates the formulation of Rajarathinam et al.[1] Compounds II and III are readily soluble in propylene glycol monomethyl ether acetate (PGMEA), which was used as the solvent throughout this study.

EXPERIMENTAL

The functionalized PNB polymer (Avatrel 8000P) was provided by Promerus LLC (Brecksville, OH).

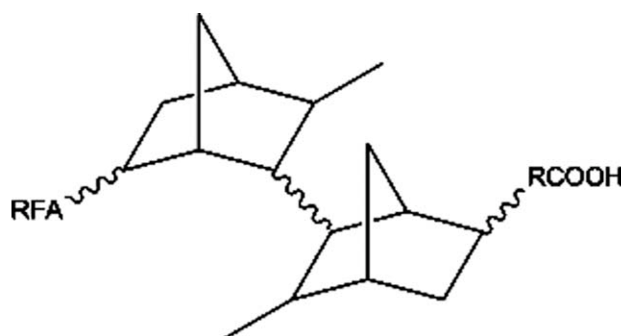

Figure 2 The chemical structure of PNB polymer (Avatrel 8000P).

TABLE I
Polynorbornene Formulations

Polymer formulation	X	Title
Base polymer	1	BF
BF with 1 wt % supplementary I	1.07	A
BF with supplementary II, III, and CPTX	1.07	B
BF with supplementary II	1.07	C
BF with supplementary III	1.07	D
BF with supplementary II and CPTX	1.07	E
BF with supplementary III and CPTX	1.07	F

The polymer mixtures were formulated by mixing a PGMEA solution of the PNB polymer with a photoacid generator (PAG), a sensitizer, and an adhesion promoter. All of the epoxy-based cross-linkers were purchased from Aldrich Chemical Co. (St. Louis, MO). A summary of the formulations made with compounds I (tetraphenylol ethane tetraglycidyl ether), II (polypropylene glycol diglycidyl ether), and III (trimethylolpropane triglycidyl ether) are listed in Table I. X is defined as the mole fraction of epoxy moieties in each formulation, where $X = 1$ in the case of BF, as was used previously.[1] In the base formulation, the value of X for compounds II, III, and adhesion promoter are 0.86, 0.09, and 0.05, respectively. The epoxy cross-linkers were dissolved in PGMEA and ball-milled with the PNB resin for 72 h. For the thick-film samples, the polymers were spin-coated on <100> silicon wafers using a CEE 100CB Spinner at 1000 rpm for 30 sec, producing $\sim$ 40-μm-thick films. The films were soft-baked at 100°C for 10 min in an oven (air ambient) to remove residual solvent. The effect of exposure dose was studied using a variable-density optical mask (Opto-Line International, Wilmington, MA). Contact printing was used to evaluate the aspect-ratio of the photodefined structures. Ultraviolet (UV) exposures were performed using a Karl Suss MA-6 Mask Aligner with a 365-nm filter. The samples were post-exposure baked in an oven at 100°C for 8 min. The thin-film samples (25 μm) were spin-coated at 1500 rpm for 30 sec. Polymers were soft-baked and hard-baked at the same conditions, which was 100°C for 5 min in an air ambient atmosphere oven. The exposed films were developed using Shipley MF-319 TMAH developer. After developing, the films were cured in a nitrogen-purged furnace at 225°C. The temperature was ramped at 5°C/min and held at temperature for 1 h. The furnace was allowed to cool slowly to ambient temperature by natural convection.

The film thickness was measured after the postexposure bake (PEB) with a Veeco Detak profilometer. Scanning electron micrograph images of the patterned films were taken using a Zeiss Ultra 60. The UV absorbance of the polymer mixtures was measured using an UV-vis spectrometer (Hewlett–Packard 8543 UV) with a quartz cuvette (1 mL working volume, 5 mm path length). Solid samples were dissolved in PGMEA. The swelling of thick-film samples was conducted using an Ohaus Voyager Pro balance with readability of 0.0001 g and linearity of ±0.0002. Fourier-transform infrared (FT-IR) spectroscopy was used to follow the epoxy ring-opening reaction using a Magna 560 spectrometer (Nicolet Instruments, Madison, WI). FT-IR scans were collected in transmission mode on KBr crystals, with 500 scans being averaged for each measurement at a resolution of 2.00 cm^{-1}. To monitor conversion, the epoxy ring-opening reaction was monitored by following the disappearance of the 844 cm^{-1} peak.

Quasistatic nanoindentation was performed on thin-film samples with a Triboindenter nanoindenter (Hysitron, Minneapolis, MN). The indenter was located on an antivibration table and enclosed in an acoustic housing. A Berkovich tip was loaded to 7500 μN in 10 sec, held for 10 sec, and unloaded to 250 μN in 2 sec. To minimize the impact of the substrate on the indentation results, the maximum force was chosen to indent less than 5% of the film thickness, which was 25 μm. Additionally, to exclude edge effects, a 5 × 5 array of points was indented in the center of the samples. The maximum drift rate of the experiments was set to 0.1 nm/sec and was determined over a period of 40 sec. The curvature of the Berkovich tip was between 250 and 970 nm. The Oliver–Pharr model was used to analyze the load–depth curves.[1] The hardness was obtained from eq. (2), and the reduced modulus was extracted from the 20% to 95% portion of the unloading curve. To eliminate the impact of thermal drift, the first data points were discarded so that the average hardness and modulus only included indents above 500 nm.

A 1 wt % solution of 3-aminopropyltriethoxy silane (3-APS) in ethanol (90% ethanol) was applied on the substrate surface in all experiments to enhance the film-to-substrate adhesion. The solution was spin-coated at 300 rpm for 10 sec followed by a higher-speed spin at 1500 rpm for 20 sec. To remove excess ethanol, the samples were baked at 130°C for 15 min on a hotplate. A 15-sec ethanol rinse was performed to remove excess materials.

High-aspect-ratio structures were fabricated on metalized silicon wafers composed of sputtered Ti/Cu/Ti (300/3000/300 Å). The metal was deposited on silicon wafers with a Unifilm sputterer. SiO_2 (1.5 μm thick) was deposited on the final titanium layer using a Unaxis PECVD to improve the film-to-substrate interface. The epoxy polymers formulations were also spin-coated using the same procedure as described above. After the samples were developed, the samples underwent a descum step using a Plasma-Therm-RIE. The final polymer thickness was

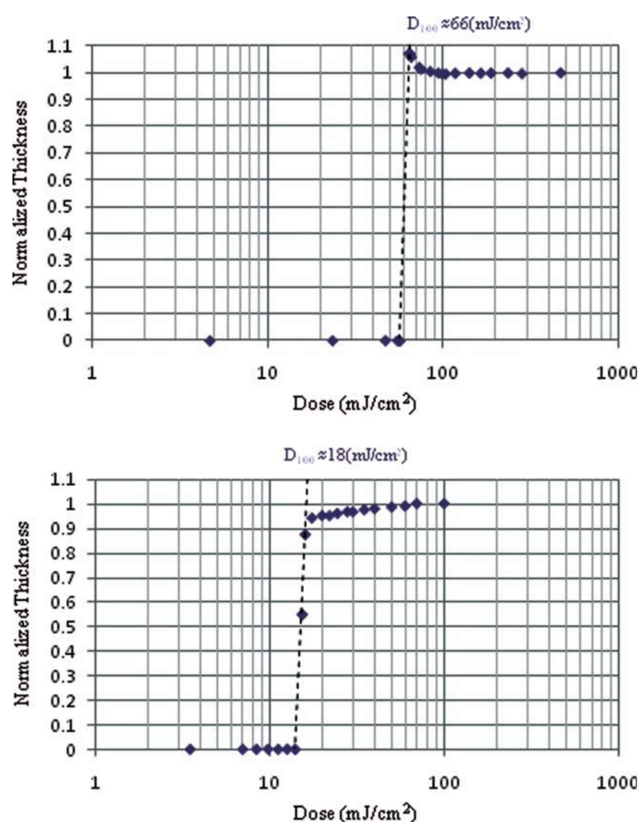

Figure 3 Contrast curve for (a) PNB-based polymer and (b) norbornene-based polymer with supplementary I. The dashed line shows the slope used to obtain the contrast.

38–40 μm. The SiO_2 and top surface of titanium were etched using buffered oxide etch for 7 min. The exposed copper surface was then suitable for electroplating copper metal in the regions where the polymer was developed away. An acid copper sulfate plating bath was used. The copper electroplating bath contained 120 g of copper sulfate ($CuSO_4 \cdot 5H_2O$) and 139 mL of sulfuric acid in 1500 mL of deionized water. The bath also contained 0.189 g of hydrochloric acid to reduce anode polarization and eliminate striated deposits and 1.134 g of polyethylene glycol as a carrier, leveler, and brightener. The current density was 10–15 mA/cm^2, yielding a plating rate of 20 μm/hr.

RESULTS AND DISCUSSION

The behavior of the three epoxy cross-linkers, I, II, and III, were studied, and their effect on the physical and photochemical properties of the BF was investigated. The photosensitivity and contrast of the BF was first evaluated. The contrast, eq. (1), describes the relationship between exposure dose and film thickness after developing.[1] Generally, high contrast is needed to make vertical-walled, high-aspect-ratio features. High contrast is achieved when an incremental increase in cross-linking leads to insolubility of the polymer film.[27] High contrast can lead to high-aspect-ratio vertical-walled structures, if adhesion of the resist to the substrate can be maintained during development of the latent image. To evaluate the impact of compound I on the sensitivity, contrast, and aspect ratio of BF, the contrast of formulation A (Table I) was compared with the contrast of BF. The mole fraction of epoxy moieties in formulation A was increased to $X = 1.07$, compared with the normalized value of $X = 1.00$ for the base formulation, by addition of 1 wt % of epoxy compound I. That is, 1 wt % of compound I (weight percent solids in the formulated solution) corresponds to 7 mol% of total epoxy in BF, making $X = 1.07$ for the final solution. Front-side, normal incident exposure was conducted, and the contrast curves are shown in Figure 3. The resulting 25-μm tall structures using formulation A had vertical side-walls, as shown in Figure 4.

The contrast values were calculated from the slope of the line in the contrast curve where there is a transition from essentially full development (film removal) to no development (full or partial film remaining). Using the slope of the line in the contrast curve, and interpolation of the values of D_0 and D_{100}, avoids possible errors in having to pick a single value for D_0 and D_{100}. Formulation A yielded a contrast of 24.2, which is exceptionally high, even compared with that for BF ($\gamma = 7.4$). This 3.3-fold improvement in contrast compared with that for BF was solely due to the 1 wt % addition of the tetrafunctional epoxy. As can be discerned from Figure 3(b), the contrast value obtained for formulation A is an accurate value as a result of multiple data points defining the slope of the contract curve between D_0 and D_{100}. It should be noted that the contrast value for BF, Figure 3(a), is a minimum contrast value

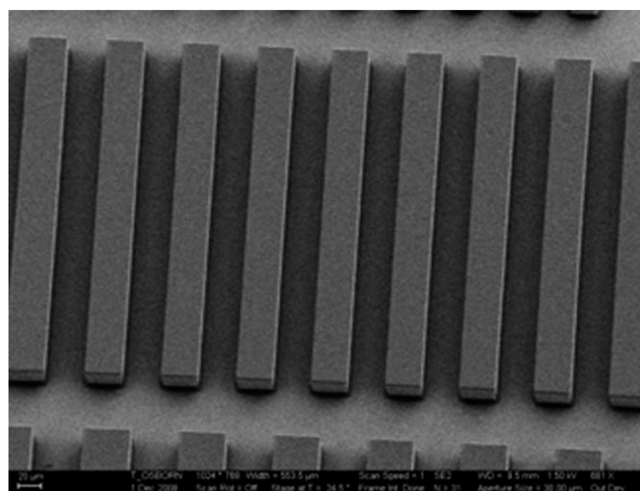

Figure 4 Scanning electron micrograph image of norbornene photopatterned with an exposure dose of 400 mJ/cm^2.

because only D_0 and D_{100} were observed. Thus, the true slope is at least as great as the value obtained by connecting D_0 and D_{100}.

In the case of BF, the value of D_{100} is at a thickness value greater than 1, and the resulting contrast is somewhat misleading because the films exposed at doses near D_{100} suffered from poor adhesion to the substrate. The value of thickness was greater than 1 in Figure 3(a) because the film delaminated from the surface at the edge of the exposed region. Rajarathinam et al.[1] showed that epoxy activation at the polymer-to-substrate interface is critical for adhesion. In front-side, normal incident exposures, the UV intensity at the surface of the film is high. However, the optical intensity at the polymer–substrate interface is attenuated by UV absorption within the film, resulting in a lower exposure dose at depths within the film. Rajarathinam et al.[1] showed this by comparing front-side and back-side exposures. If the top surface is exposed to doses at or near D_{100}, then the exposure dose at the polymer–substrate interface will be below D_{100}, especially for thick-film samples.

The absorption of UV radiation results in activation of the PAG and creation of an acid, which initiates epoxy ring opening and polymer cross-linking. The lower exposure dose at the polymer–substrate interface results in fewer epoxy units being activated at the wafer surface and can lead to poor adhesion and delamination. The addition of compound I to the BF, as in formulation A, increases the optical density (OD) of the film at 365 nm. The optical intensity of the incident UV radiation for formulation A at the polymer–substrate interface was less than that of BF because of the increased absorption of compound I within the film. Thus, the superior adhesion of formulation A must be due to the presence of the tetrafunctional epoxy, compound I, (within the film and at the polymer–substrate interface) and its higher efficacy for producing adhesion, compared with the other epoxy compounds used in BF.

The addition of the tetrafunctional epoxy, compound I, affected the solubility of the unexposed film in the aqueous-base developer. The developing time for formulation A was 4.50 min compared with 3.00 min for BF. The increased adhesion and longer developing time with formulation A could have been due to fractional epoxy ring opening after spin-coating and baking (soft-bake and PEB). This was investigated in unexposed samples using FT-IR spectroscopy. The FT-IR peak corresponding to the epoxy rings (844 cm^{-1}) showed a 12% decrease after PEB (with no exposure) compared with the same film after spin coating (no exposure or baking steps), showing that some of the epoxide rings had reacted, resulting in some degree of cross-linking in the unexposed regions after the 100°C bake. Epoxy ring opening can occur during thermal treatments or can be acid activated, if some of the PAG was thermally activated. It was also noted that the less swelling occurred in the exposed regions of formulation A, compared with BF, which will be discussed in more detail later in the article when swelling is discussed. Enhanced epoxy ring opening and polymer cross-linking was also seen, as shown later in the FT-IR data.

The sensitivity or photospeed of the polymer is a critical attribute of each formulation. The absorption of UV radiation within the polymer film results in activation of the PAG producing an acid within the polymer film. The photogenerated acid catalyzes epoxy ring-opening reaction, which leads to PNB cross-linking. The absorption of UV radiation can be increased by adding a sensitizer to the polymer formulation, as was done with BF. Energy transfer occurs between the sensitizer and the PAG, creating the acid catalyst. However, the sensitizer does not participate in polymer cross-linking and remains in the polymer film as a low-molecular-weight additive.

The sensitivity of the polymer mixture is the minimum exposure dose to obtain photodefinition at a fixed developing condition. The D_{100} value, obtained from the contrast curves, was improved from 66 mJ/cm^2 for BF to 18 mJ/cm^2 for formulation A. Thus, UV radiation is significantly more effective at activating the PAG and initiating cross-linking after PEB, when the tetrafunctional epoxy, I, is present.

To evaluate the impact of compound I on the polymer sensitivity at 365 nm, a series of UV absorption experiments were conducted. The absorbance of PGMEA, BF, and dilute solutions of I, II, and III in PGMEA were measured in the UV and visible regions. PGMEA, II, and III had very low absorbance at wavelengths from 300 to 400 nm. Compound I was found to have high molar absorptivity in the UV. The absorptivity of compound I in PGMEA was compared with the absorptivity of a dilute solution of the sensitizer used in BF, 1-chloro-4-propoxy-9H-thioxanthen-9-one (CPTX), in PGMEA, as shown in Figure 5. The molar absorbance of I and CPTX are 172,287 and 395,779 L mol^{-1} m^{-1}, respectively.

The higher absorbance of formulation A, compared with BF, by itself does not account for the improved adhesion and sensitivity of the tetrafunctional epoxy. In the case of a partially cross-linked polymer, a higher degree of functionality within the cross-linker will lead to a higher degree of cross-linking in the polymer film. That is, the overall cross-link density using compound I will be higher than that of compound II or III, for a given mole fraction of epoxy moieties, when the films are partially cured (same degree of curing) because compound I has a higher degree of functionality. Thus, the higher cross-link density of the tetrafunctional

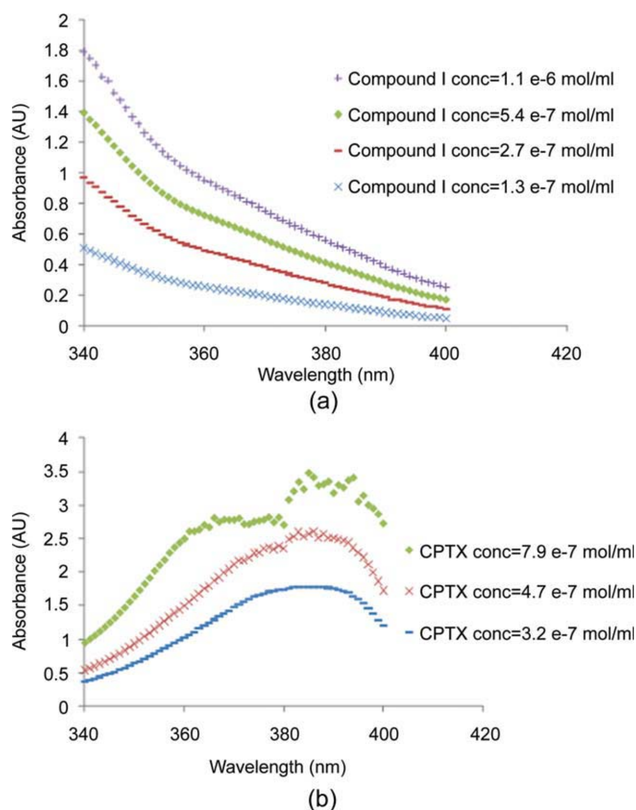

Figure 5 Changes in UV-vis spectrum of dilute solution of (a) I and (b) CPTX, in PGMEA from 200 to 600 nm. [Color figure can be viewed in the online issue, which is available at wileyonlinelibrary.com.]

epoxy is an asset when the film is partially cross-linked, as in the case of soft baked or postexposure baked films. This point will be revisited in greater detail later in the article.

These results show that the increase in the sensitivity of formulation A, compared with BF, is at least partly due to the higher absorbance of compound I at 365 nm and subsequent activation of the PAG and creation of the acid catalyst, compared with the other epoxy compounds. To compare the effect of simply adding more epoxy to BF, polymer formulations containing an identical quantity of epoxy moieties, using II and III, were studied. Formulation B was prepared so as to contain the exact number of equivalents of epoxy as formulation A. Because compound I has a higher molar absorptivity than compounds II or III, CPTX was added to formulation B so that the new mixture had the same absorbance at 365 nm as A. Thus, B had the same mole ratio of epoxy as A and identical absorbance at 365 nm because of the additional CPTX. As shown in Figure 6, the sensitivity of B was evaluated by measuring D_{100}, which was 18 mJ/cm^2, essentially the same as formulation A. Thus, the improved sensitivity of formulation A, compared with BF, was due to the higher OD of the tetrafunctional epoxy, and subsequent energy transfer with the PAG creating the acid catalyst. The relative efficiency for energy transfer between compound I and PAG versus CPTX and PAG could have been different, but was beyond the scope of this study.

The contrast for formulation B was measured to be $\gamma = 9.96$, which is higher than BF, because of the added epoxy and CPTX; however, it is lower than that of formulation A, $\gamma = 24.2$. This result is congruent with the previous observation that the higher contrast obtained with formulation A is not simply because of a higher epoxy content or higher absorbance of the tetrafunctional epoxy. The addition of compound I did provide greater surface adhesion and swelling resistance in the cross-linked regions of the film. The improved adhesion is critical to extending the developing time and allowing full development of the features, especially at exposure doses at or just greater than D_{100}. For example, the developing time needed for formulation A was 4.50 min, compared with 3.33 min for formulation B and 3.00 min for BF. The longer developing time for formulation B, compared with BF, is attributed to a modest degree of cross-linking from the addition of II and III. Also, it improves the adhesion at the film-to-substrate interface in the exposed regions. The poor adhesion at doses just above D_{100} was visually observed in the films and is reflected in Figures 3(a) and 6. In Figure 6, the thickness values greater than 100% thickness at doses just above D_{100} correspond to delaminated films. The poor adhesion at D_{100} observed with the BF formulation was improved in formulation B by addition of epoxy compounds II and III.

The ability to make high-aspect-ratio features is a function of the contrast, adhesion characteristics, and sensitivity of a photodefinable material. Because the addition of 1 wt % of compound I had a

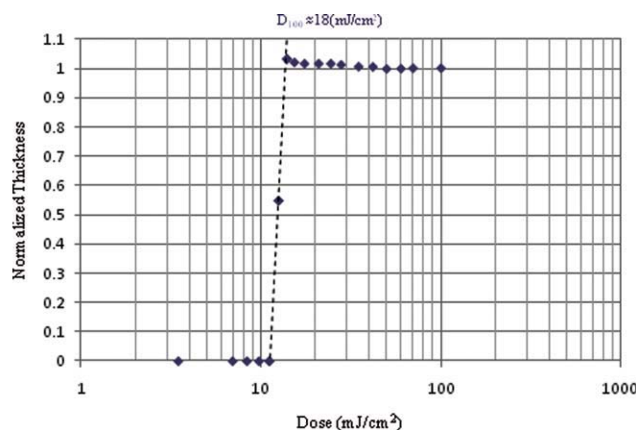

Figure 6 Contrast curve for norbornene-based polymer with supplemented CPTX, II, and III.

significant effect on these parameters in formulation A, the ability to form high-aspect-ratio features was investigated. Hollow-core structures were chosen for this work because they are the difficult to fabricate since the transport of developer into the core of the structure is restricted, compared with the transport of developer to the outside of the structure. Films were spin-coated at 1000 rpm and photopatterned at an exposure dose of 200 mJ/cm^2 at 365 nm, resulting in 38.7-μm tall, hollow-core, triangular-shaped structures. Dissolving the unexposed polymer from the region at the center of the structure before delamination occurred at the outside edge of the polymer structure is a critical test of adhesion. To confirm complete development of the center core region, copper was electroplated in the hollow core portions of the film after a 2-min plasma (RIE) descum. If the polymer was not fully developed from the center core, electroplating would not occur. Hollow-core features, 38.7-μm thick with 3-μm diameter (length of a side) opening, were fabricated using formulation A. The resulting aspect ratio was 13 : 1. The center core of the structures was fully developed because copper electroplating was observed in the center region after development. The electroplated copper filled the center region of the cavity. The polymer shell around the copper was removed, and the sidewall of the copper features was examined. The sidewalls were relatively straight-walled in comparison with the results reported previously by Rajarathinam et al.[1] For comparison, 13 : 1 aspect-ratio structures were formed with BF at a higher exposure dose of 400 mJ/cm^2, and 11 : 1 aspect-ratio hollow structures were made with formulation B at an exposure dose of 200 mJ/cm^2. The same process as above was performed; however, incomplete developing occurred in the cavities of both BF and formulation B, as shown by a lack of copper plating. In both cases, longer developing time was needed to fully develop the center core, which led to film delamination and lifting because of the lack of film-to-substrate adhesion. Thus, only formulation A had sufficient adhesion and contrast to produce features with aspect ratio greater than 13 : 1. It can be concluded that 1 wt % of compound I improved the contrast, sensitivity, and film-to-substrate adhesion of formulation A and led to higher aspect-ratio features with straight side-walls and high fidelity.

The reduced modulus and hardness of BF and formulations A and B were compared using nano-indentation. All samples were tested after a 225°C cure for 1 h. Formulations A, BF, and B had a reduced modulus of 2.80, 2.82, and 2.83 GPa, respectively. The hardness values for A, BF, and B were 0.17, 0.16, and 0.18 GPa, respectively. This shows that no significant change in mechanical properties occurred because of the additional epoxy-based cross-linkers in formulations A and B.

The extent of cross-linking can play an important role in the properties of the polymer.[29,30] To evaluate the effect of compounds I, II, and III on the cross-link density of the cured polymer, the average molecular weight between cross-links (M_c) and effect of cross-link functionality (f_c) were calculated and compared assuming fully reacted and cross-linked films. In addition, two formulations were made to experimentally compare the effect of cross-linking (Table I). In one case, formulation C, compound II was added to BF to provide an equivalent number of epoxide groups as in formulation A. In the second case, formulation D, compound III was added so that the total molar epoxy content was the same as formulation A. The values of M_c and f_c were calculated using eqs. (5) and (6), which assumes that all the epoxy moieties have reacted and each has resulted in backbone cross-linking.

$$M_c = \frac{2(M_e + \sum_{f=2}^{\infty} \frac{M_f}{f} \Phi_f)}{\sum_{f=3}^{\infty} \Phi_f} \tag{5}$$

$$f_c = \frac{\sum_{f=3}^{\infty} \Phi_f}{\sum_{f=3}^{\infty} (\frac{\Phi_f}{f})} \tag{6}$$

where M_e is the epoxide equivalent weight of the resin, f is the functionality of the cross-linker, M_f is the molecular weight of the f-th functional cross-linker, and Φ_f is the mole fraction of epoxy moles provided by the f-th functional cross-linker.[31,32]

With full conversion of the cross-linkers, M_c and f_c were calculated. The calculated network parameters are summarized in Table II. In the work of Crawford and Lesser,[31] full conversion was achieved. That is, the calculation assumes that all polymer sites were reacted with epoxy groups, and no cross-linking occurred between epoxy groups.

The results show that there is little difference between the M_c and f_c values for the various formulations. This implies that compounds I, II, and III could each result in nearly the same cross-link density. This result is consistent with the mechanical property measurements shown above where the properties for the formulations with compounds I, II, and III are essentially identical. As shown in Table II, the model predicts a similar average molecular weight between cross-links for BF and the other formulations with slightly higher epoxy content. In the films, this occurs because there are enough sites on the polymer backbone for complete cross-linking for all the epoxy units in each formulation. Thus, the addition of a small amount of epoxy does not

TABLE II
Network Properties

Formulations	M_c (gr/mol)	f_c
BF	446	3
A	449	3
C	491	3
D	441	3

change M_c by very much. This will be confirmed in the next section where it is shown that the solvent swelling within the polymer is a function of the mole fraction of epoxy only, and not the functionality of the different epoxy additives. The M_c value obtained for formulation C is slightly higher than the other formulations because of the higher molecular weight per epoxy moiety for compound II compared with compounds I and III. The same M_c value would be obtained for all formulations with the same mole fraction of epoxy, if the molecular weight per epoxy functionality for the different cross-linkers was identical.

Swelling experiments were performed to investigate the actual degree of cross-linking. A larger value of M_c (lower degree of cross-linking) will result in greater solvent swelling.[30] Swelling tests were performed in PGMEA. Formulations were made so that the molar content of epoxide and OD were constant for the different experiments. The optical absorbance of epoxies II and III was less than that of compound I. Thus, CPTX was added to formulations with II and III so that the formulations had the same OD. Formulations E and F, Table I, have the same molar quantities of epoxy and OD as formulation A. The swellings of BF, A, E, and F were measured after PEB and final cure. Each sample was cured for 1 h at 225°C followed by soaking in PGMEA. The mass of each sample was measured at six different times during the 24-hr swelling period. The percent increase in weight was calculated from eq. (7) and is shown in Figure 7. Each data point is the average of four measurements. The average of standard deviation was less than 0.0003.

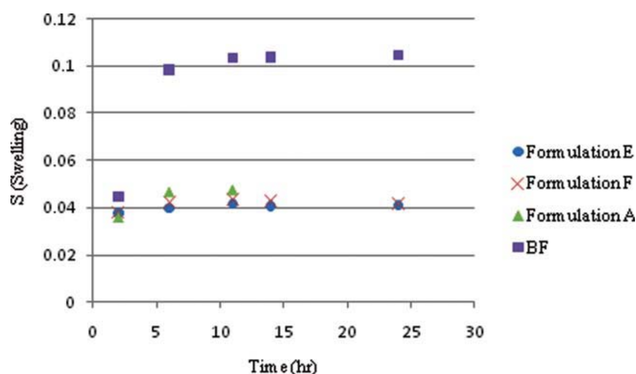

Figure 7 Influence of difunctional, trifunctional, and tetrafunctional cross-linker on swelling of fully cross-linked cured polymer. [Color figure can be viewed in the online issue, which is available at wileyonlinelibrary.com.]

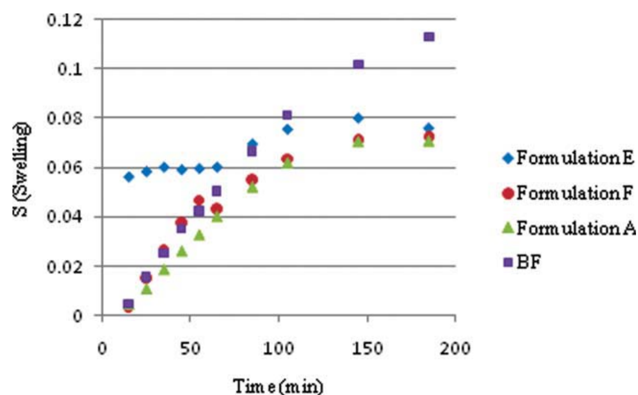

Figure 8 Influence of difunctional, trifunctional, and tetrafunctional cross-linker on swelling of cross-linked baked polymer. [Color figure can be viewed in the online issue, which is available at wileyonlinelibrary.com.]

$$S = \frac{W_t - W_0}{W_0} \quad (7)$$

where S is the swelling and W_t is the weight of sample swollen with solvent at time t, and W_0 is the sample weight in dry state.[33,34]

Figure 7 shows an increase in weight with swelling time. No significant difference was found between the various formulations when the epoxy content was identical. This agrees with the calculation of M_c for the different formulations. That is, each epoxy compound resulted in a similar degree of cross-linking. The degree of swelling was greater for BF because it has a slightly lower molar epoxy content than the other formulations. In the model calculations above, it was assumed that all the polymer reaction sites were fully reacted through an epoxy reaction with the cross-linkers. However, there is an excess of reactive sites on the polymer so that after reaction with the epoxy, unreacted sites will remain on the polymer. The addition of a cross-linker to the polymer increases the degree of cross-linking between the epoxy and the polymer reaction sites, regardless of the functionality of the cross-linker.

The swelling tests were replicated after PEB, as shown in Figure 8. As in Figure 7, there was no swelling dependence on cross-linker functionality. However, a high degree of film lifting and delamination occurred across the film for formulation F. A lower degree of delamination around the corners of the film was observed for formulation E. Because of the adhesion improvement with compound I, no delamination of formulation A was observed anywhere on the silicon surface. The diversity in the degree of delamination observed for compounds I, II, and III shows the complex nature of adhesion

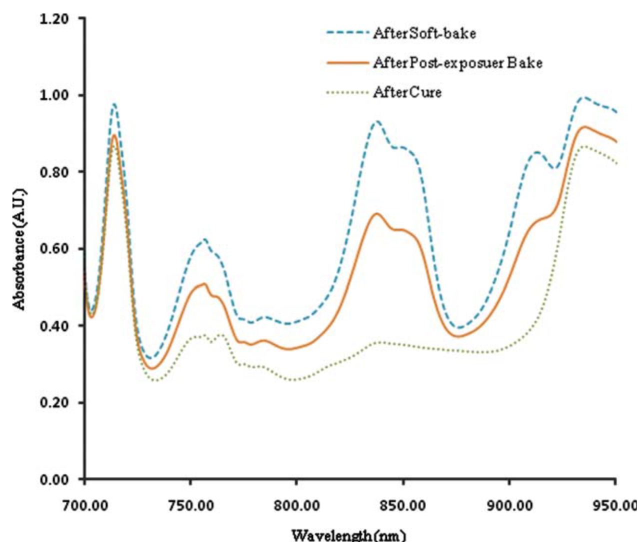

Figure 9 Change in FT-IR spectrum of the thin-film BF from 700 to 950 cm^{-1} as a function of processing steps (soft-bake: 100°C for 5 min; exposure: 250 mJ/cm^2; postexposure bake: 100°C for 5 min; and cure: 1 h at 225°C). [Color figure can be viewed in the online issue, which is available at wileyonlinelibrary.com.]

caused by the epoxy reaction for PNB and epoxy cross-linkers.

To study the reactivity of the cross-linkers, the degree of epoxy ring opening for formulations BF, A, and E after PEB was investigated using FT-IR spectroscopy. All formulations show epoxy ring opening after PEB, suggesting that some cross-linking has occurred. The IR spectra for the thin-film BF from 700 to 950 cm^{-1} are shown in Figure 9. The FT-IR peak corresponding to epoxy was not observed after curing at 225°C in all cases showing that the epoxide rings had reacted, resulting in adequate adhesion after curing for all formulations. The exact nature of the improved adhesion for compound I, beyond its higher epoxy functionality and absorbance, was not investigated and may be the subject of future publication. Even though the cross-linkers show the same degree of swelling resulting in the same cross-link density, they result in a significantly different degree of adhesion. These observations confirm the results obtained from previous experiments; excellent film–substrate adhesion can be obtained by the addition of small amount of tetrafunctional epoxy at the 1 wt % level.

CONCLUSIONS

The tetrafunctional epoxy-based cross-linker, I, showed a significantly different behavior compared with the difunctional, II, and trifunctional, III, cross-linkers studied. The tetrafunctional epoxy cross-linker, I, showed a high UV absorption between 250 and 400 nm, and the sensitivity of the polymer with 1 wt % additional I was enhanced by a factor of 3.7. A minor increase in the contrast of the base polymer was observed by addition of difunctional and trifunctional cross-linkers, whereas the contrast value of the base polymer, 7.36, was increased to 24.2 due to addition of 1 wt % tetraphenylol ethane tetraglycidyl ether. The base polymer with supplemental tetrafunctional cross-linker shows excellent adhesion at the film–substrate interface, enabling the fabrication high-aspect ratio structures (13 : 1 aspect ratio) with high-fidelity and straight side-walls photodefined structures. The addition of the tetrafunctional cross-linker to the base polymer resulted in high contrast, high sensitivity, excellent adhesion, and the ability to make high-aspect-ratio features, making the polymer films suitable for MEMS and microelectronics applications.

References

1. Rajarathinam, V.; Lightsey, C. H.; Osborn, T.; Knapp, B.; Elce, E.; Allen, S. A. B.; Kohl, P. A. J Electron Mater 2009, 38, 778.
2. Liu, C. Adv Mater 2007, 19, 3783.
3. Wang, X.; Engel, J.; Liu, C. J Micromech Microeng 2003, 13, 628.
4. Bai, Y. Q.; Chiniwalla, P.; Elce, E.; Shick, R. A.; Sperk, J.; Allen, S. A. B.; Kohl, P. A. J Appl Polym Sci 2004, 91, 3023.
5. Lorenz, H.; Laudon, M.; Renaud, P. Microelectron Eng 1998, 41, 371.
6. Wei, X.; Lee, C.; Jiang, Z.; Jiang, K. Proc Inst Mech Eng C: J Mech Eng Sci 2008, 222, 37.
7. Briscoe, B. J.; Fiori, L.; Pelillo, E. J Phys D Appl Phys 1998, 31, 2395.
8. Lee, C.; Jiang, K. KMPR Photoresist for Fabrication of Thick Microstructures; Proceedings of the 3rd International Conference on Multi-material Micro Manufacture, 2007; pp 207–210.
9. Bai, Y. Q.; Chiniwalla, P.; Elce, E.; Allen, S. A. B.; Kohl, P. A. J Appl Polym Sci 2004, 91, 3031.
10. Chiniwalla, P.; Bai, Y. Q.; Elce, E.; Shick, R.; McDougall, W. C.; Allen, S. A. B.; Kohl, P. A. J Appl Polym Sci 2003, 89, 568.
11. Chiniwalla, P.; Bai, Y. Q.; Elce, E.; Shick, R.; Allen, S. A. B.; Kohl, P. J Appl Polym Sci 2004, 91, 1020.
12. Feng, R.; Farris, R. J Micromech Microeng 2003, 13, 80.
13. Lee, C.; Jiang, K. J Micromech Microeng 2008, 18, 055032.
14. Bogdanov, A.; Peredkov, S. Microelectron Eng 2000, 53, 493.
15. LaBianca, N.; Gelorme, J. Proc SPIE 1995, 2438, 846.
16. Gelorme, J.; Cox, R.; Gutierrez, S. U.S. Pat. 4,882,245.1989.
17. Ruhmann, R.; Pfeiffer, K.; Falenski, M.; Reuther, F.; Engelke, R.; Grützner, G. NEXUS-Network of Excellence in Multifunctional Microsystems EUROPRACTICE-Microsystems Service for Europe, SU-8 - a high performance material for MEMS applications, Polymers in MEMS, 2002, pp 45–46.
18. Lee, K.; LaBianca, N.; Rishton, S.; Zolgharnain, S.; Gelorme, J.; Shaw, J.; Chang, T. J Vac Sci Technol B 1995, 13, 3012.
19. Lin, C.; Lee, G.; Chang, B.; Chang, G. J Micromech Microeng 2002, 12, 590.
20. LaBianca, N. C.; Gelorme, J. D.; Lee, K. Y.; Sullivan, E. O.; Shaw, J. M. Electrochem Soc 1993, 95, 386.
21. Liu, G.; Tian, Y.; Kan, Y. Microsyst Technol 2005, 11, 343.
22. Bertsch, A.; Lorenz, H.; Renaud, P. IEEE J Microelectromech Syst 1998, 7, 18.
23. Despont, M.; Lorenz, H.; Fahrni, N.; Brugger, J.; Renaud, P.; Vettiger, P. In Proceedings of IEEE MEMS'96, San Diego, CA; 1996; pp 162–167.
24. Lorenz, H.; Despont, M.; Fahrni, N.; LaBianca, N.; Renaud, P.; Vettiger, P. J Micromech Microeng 1997, 7, 121.

25. Dellmann, L.; Roth, S.; Beuret, C.; Racine, G.; Lorenz, H.; Despont, M.; Renaud, P.; Vettiger, P.; De Rooij, N. Sensors Actuators A: Phys 1998, 70, 42.
26. Guériti, L.; Bosse, M.; Dcmierre, M.; Calmes, S.; Renaud, P. Simple and low cost fabrication of embedded microchannels by using a new thick-film photo-plastic, IEEE, Vol. 2, 1997, pp 1419–1422.
27. May, G.; Spanos, C. Fundamentals of Semiconductor Manufacturing and Process Control; Wiley-IEEE Press: New York, 2006.
28. Oliver, W.; Pharr, G. J Mater Res 1992, 7, 1564.
29. Mark, J. Rubber Chem Technol 1982, 55, 762.
30. Soh, M.; Yap, A. J Dentistry 2004, 32, 321.
31. Crawford, E.; Lesser, A. J Polym Sci Part B: Polym Phys 1998, 36, 1371.
32. Thompson, Z.; Hillmyer, M.; Liu, J.; Sue, H.; Dettloff, M.; Bates, F. Macromolecules 2009, 42, 2333.
33. Yao, K.; Peng, T.; Feng, H.; He, Y. J Polym Sci Part A: Polym Chem 1994, 32, 1213.
34. Bigi, A.; Cojazzi, G.; Panzavolta, S.; Rubini, K.; Roveri, N. Biomaterials 2001, 22, 763.